Key role of NO3 radicals in the production of isoprene nitrates and nitrooxyorganosulfates in Beijing

Article

Accepted Version

Hamilton, J. F. ORCID: https://orcid.org/0000-0003-0975-4311, Bryant, D. J., Edwards, P. M., Ouyang, B. ORCID: https://orcid.org/0000-0001-8663-1935, Bannan, T. J. ORCID: https://orcid.org/0000-0002-1760-6522, Mehra, A., Mayhew, A. W. ORCID: https://orcid.org/0000-0001-5277-1331, Hopkins, J. R., Dunmore, R. E., Squires, F. A., Lee, J. D., Newland, M. J., Worrall, S. D. ORCID: https://orcid.org/0000-0003-1969-3671, Bacak, A., Coe, H., Percival, C. ORCID: https://orcid.org/0000-0003-2525-160X, Whalley, L. K., Heard, D. E. ORCID: https://orcid.org/0000-0002-0357-6238, Slater, E. J., Jones, R. L., Cui, T., Surratt, J. D. ORCID: https://orcid.org/0000-0002-6833-1450, Reeves, C. E., Mills, G. P., Grimmond, S. ORCID: https://orcid.org/0000-0002-3166-9415, Sun, Y., Xu, W., Shi, Z. ORCID: https://orcid.org/0000-0002-7157-543X and Rickard, A. R. (2021) Key role of NO3 radicals in the production of isoprene nitrates and nitrooxyorganosulfates in Beijing. Environmental Science and Technology, 55 (2). pp. 842-853. ISSN 1520-5851 doi: https://doi.org/10.1021/acs.est.0c05689 Available at https://centaur.reading.ac.uk/95950/

https://dx.doi.org/10.1021/acs.est.0c0568 Environ. Sci. Technol. 2021, 55, 842−8539

Key Role of NO_3 Radicals in the Production of Isoprene Nitrates and Nitrooxyorganosulfates in Beijing

Jacqueline F. Hamilton, DJ Bryant, Peter M. Edwards, Bin Ouyang, Thomas J. Bannan, Archit Mehra, Alfred W. Mayhew, James R. Hopkins, Rachel E. Dunmore, Freya A. Squires, James D. Lee, Mike J. Newland, Stephen D. Worrall, Asan Bacak, Hugh Coe, Carl Percival, Lisa K. Whalley, Dwayne E. Heard, Eloise J. Slater, Roderic L. Jones, Tianqu Cui, Jason D. Surratt, Claire E. Reeves, Graham P. Mills, Sue Grimmond, Yele Sun, Weiqi Xu, Zongbo Shi, and Andrew R. Rickard*

ABSTRACT: The formation of isoprene nitrates (IsN) can lead to significant secondary organic aerosol (SOA) production and they can act as reservoirs of atmospheric nitrogen oxides. In this work, we estimate the rate of production of IsN from the reactions of isoprene with OH and NO3 radicals during the summertime in Beijing. While OH dominates the loss of isoprene during the day, NO3 plays an increasingly important role in the production of IsN from the early afternoon onwards. Unusually low NO concentrations during the afternoon resulted in NO3 mixing ratios of ca. 2 pptv at approximately 15:00, which we estimate to account for around a third of the total IsN production in the gas phase. Heterogeneous uptake of IsN produces nitrooxyorganosulfates (NOS). Two mononitrated NOS were correlated with particulate sulfate concentrations and appear to be formed from sequential NO3 and OH oxidation. Di- and tri-nitrated isoprene-related NOS, formed from multiple NO3 oxidation steps, peaked during the night. This work highlights that NO3 chemistry can play a key role in driving biogenic−anthropogenic interactive chemistry in Beijing with respect to the formation of IsN during both the day and night.

INTRODUCTION

Poor air quality is the biggest environmental factor contributing to premature mortality globally.(1) As earth's population has grown, the number of people living in urban areas has increased rapidly from 751 million in 1950 to 4.2 billion in 2018.(2) By 2030, the UN estimates that there will be 43 megacities (>10 million inhabitants), with most of them located in developing countries in Africa, Asia, and Latin America.(2) Since many of these locations are situated in the tropics, high average temperatures can lead to significant emissions of biogenic volatile organic compounds (BVOC) to the urban atmosphere, in particular isoprene.(3) Beijing, China, is a well-studied megacity, with significant air quality issues related to particle pollution and ozone (O3) production. Beijing experiences high average summertime temperatures (ca. 30 °C) and has a high percentage of urban green space (>41% urban green space),(4) which can lead to significant amounts of isoprene being emitted.(5) Photochemical oxidation of isoprene in the presence of high levels of anthropogenic pollutants, in particular nitrogen oxides (NOx) and sulfur dioxide (SO2), can lead to enhanced secondary organic aerosol (SOA) production.(6−21)

A key uncertainty in understanding SOA production from isoprene is the role of isoprene nitrates (IsN). IsN are formed in chain-terminating reactions during oxidation by hydroxyl radicals (OH) in the presence of NO or by nitrate radicals (NO_3). IsN formation can reduce local O_3 production and acts as a sink for atmospheric nitrogen.(22) During the daytime, the reaction of isoprene with OH leads to the formation of hydroxy peroxy radicals (ISOPOO), which can react with NO to form isoprene hydroxy nitrates (IHN), with further reactions leading to a suite of multifunctional IsN species (see Wennberg et al. and references therein).(23) At night, OH radical concentrations are much lower,

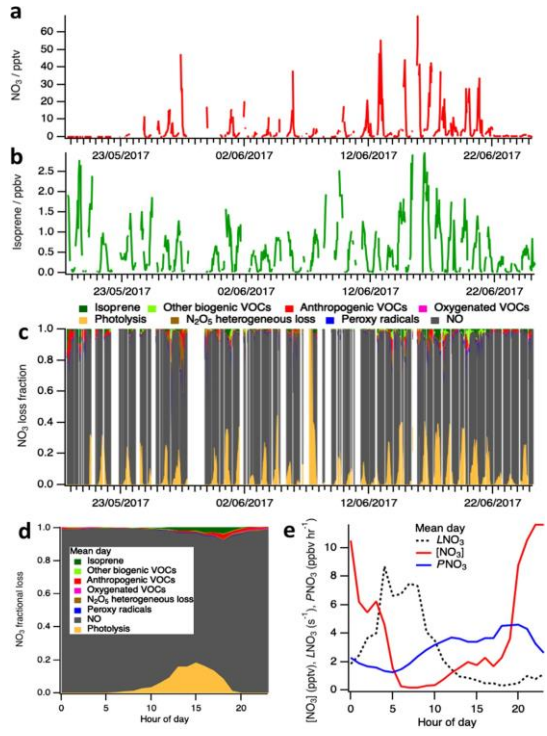

Figure 1. (a) Time series of NO_3 mixing ratio (pptv) measured by the BBCEAS. (b) Time series of isoprene (ppbv) measured by DC-GC-FID. (c) NO_3 loss fraction calculated using measured NO_3 sinks, including photolysis and heterogeneous losses. N_2O_5 aerosol uptake coefficient of 0.022 has been used based on Tham et al.[49] (d) Mean diurnal variation of data shown in (c). (e) Mean diurnal variation of NO_3 mixing ratio (pptv), total production (P_{NO_3}), and loss rates (L_{NO_3}) (ppbv h^{-1} and s^{-1}, respectively). VOCs in each classification are given in Table S1.

and in areas with sufficient NO_x to form NO_3 rapidly,[24] oxidation by NO_3 radicals often becomes a more important route for loss of isoprene. Reaction with NO_3 leads to the production of isoprene nitrooxy peroxy radicals (INO_2), which can then go on to form a range of IsN species via reactions with HO_2, RO_2, and NO.[25,26] During the daytime, volatile organic compound (VOC) + NO_3 reactions are usually limited by the fast photolysis of NO_3 and its reaction with NO.

IsN have recently been observed in rural and forested regions using online chemical ionization mass spectrometry. Ayres et al. measured organic nitrates at a rural forested site in Alabama as part of the SOAS campaign, where emissions were dominated by biogenic VOCs.27 They identified a number of IsN (C5H9NO5, C5H9NO4, C4H9NO5) and they were mainly found in the gas phase. Massoli et al. identified highly oxygenated molecules (HOMs) from isoprene during the same project.28 Significant amounts of highly oxidized IsN were also identified, with some species having a strong correlation with SO2 mixing ratios in anthropogenically impacted air masses, highlighting the importance of NOxdriven chemistry. Lee et al. identified highly functionalized IsN in organic aerosol with molecule formulas in the range

$C_5H_{7,9,11}NO_{4-9}$.[29] Similar species were also found in rural Germany in both the gas and particle phases.[30] These IsN contributed more mass in the daytime compared to the monoterpene nitrates that contributed more at night-time. Modeling the formation routes shows that while IsN formation from RO_2 + NO leads to more particulate IsN during the day, NO_3 chemistry is still an important formation route, representing around a third of the total particulate IsN at 15:00. However, the low levels of NO_3 radicals when isoprene was high made it difficult to optimize the model.

Recent observations in a boreal forest by Liebmann et al.[31] under low-NO conditions indicated that daytime alkyl nitrate production from NO_3 chemistry can dominate over OH under certain conditions. Although Beijing (and other megacities) may not be an obvious low-NO environment, recent observations indicate that in summer, NO levels in the afternoon can often drop to below 1 ppbv, and on some days <0.1 ppbv, as a result of reactions with ozone and other unknown chemical reactions.[32] Thus, daytime nitrate production from NO_3 could be important in other megacities that also experience low NO conditions during the day and high VOC levels. There are few measurements of speciated IsN in urban cities, where isoprene can be emitted from urban plants and green spaces.[22,33,34] In this paper, we show that NO_3 radical chemistry is important for the production of IsN in Beijing during summer, both during the day and at night, using a comprehensive suite of gas- and particle-phase chemical observations taken as part of U.K.−China Atmospheric Pollution and Human Health in a Chinese Megacity (APHH-China) program during the summer of 2017.

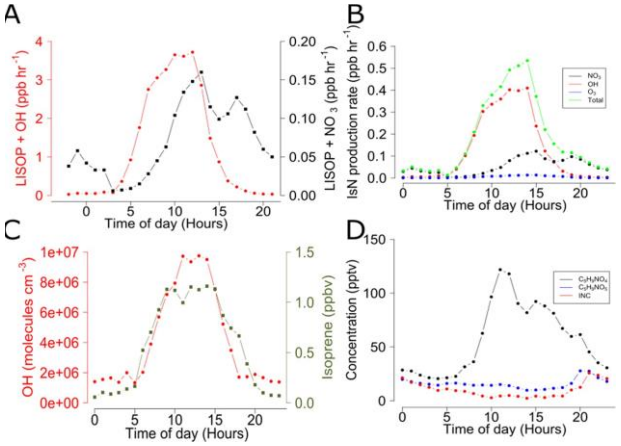

Figure 2. Average diurnal of (A) isoprene loss rate to NO_3 (black) and OH (red) in ppbv h^{-1}. (B) Calculated IsN production rate from O_3 (blue), NO_3 (black), OH (red), and total (green). (C) OH concentration (red, molecules cm^{-3}, measured by FAGE) and isoprene mixing ratio (green, ppb, measured by DC-GC-FID). (D) $C_5H_9NO_5$ (blue) and $C_5H_9NO_4$ (black) measured by I-CIMS and the sum of cis (Z) and trans (E) δ-[1,4] and δ-[4,1]-isoprene carbonyl nitrates (INC, red) was measured by GC-NI-MS. See the SI for a discussion of the calibration of I-CIMS ions.

MATERIALS AND METHODS

Time-resolved aerosol filter samples were collected between May 18 and June 24, 2017 at the Tower Section of the

Institute of Atmospheric Physics (IAP) in Beijing, China.[35] The site is typical of central Beijing, with several roads nearby, a canal to the south, and several areas of green space to the south and east. Three aerosol filter samples were collected for 3-h integrated periods between 08:30 and 17:30, and one additional sample taken overnight (17:30−08:30); see Table S2 for sampling times. Samples were collected at a height of 8 m on top of a building at the IAP complex. The samples were collected on preconditioned (500 °C for 5 h) quartz filters (8 × 10 $in.^2$) using an ECOTECH HiVOL 3000 with a selective $PM_{2.5}$ inlet. Filter samples were extracted in the laboratory into high-purity water and analyzed using an Ultimate 3000 ultra pressure liquid chromatography coupled to a Q-Exactive Orbitrap MS, with heated electrospray ionization (UPLC-ESIMS^2) using the method described in Bryant et al.[36] Further details on the method used for extraction, analysis, and calibration can be found in the Supporting Information (SI). It should be noted that using surrogate standards for calibration can lead to uncertainties, but authentic organosulphate (OS) standards with similar retention times have been used in this study to minimize this effect.[37−39] Based on the previous investigation of the ionization efficiency of organosulfates and matrix effects from aerosol samples, we estimate a total uncertainty of 60% on NOS concentrations.[36] A time-of-flight chemical ionization mass spectrometer (ToF-CIMS) using an iodide ionization system was used to measure gas-phase isoprene nitrates in real time.[40] Isoprene carbonyl nitrate (INC) was measured using gas-chromatography negative-ionization mass spectrometry (GC-NIMS).[41,42] Nitric oxide (NO) was measured via chemiluminescence with a Thermo Scientific 42i Trace Level NO_x analyzer with a limit of detection <50 ppt (120 s averaging time). NO_2 was measured via a cavity attenuated phase shift (CAPS) spectrometer (Teledyne T500U CAPS Trace-level NO_2 analyzer; the limit of detection was <40 ppt, averaging time, 60 s). Volatile organic compounds (VOCs) were measured hourly using dual-channel gas chromatography with flame ionization detection (DC-GC-FID)[43] with a limit of detection in the 1−5 ppt range. The sum of monoterpenes was measured using a proton transfer mass spectrometer (PTR-MS).[44] Measurements of OH, HO_2, and RO_2 radicals were made via two fluorescence assay by gas expansion (FAGE) detection cells.[45,46] The limits of detection (LOD) on average for the campaign were 5.5×10^5 molecules cm^{-3} for OH and 3.1×10^6 molecules cm^{-3} for HO_2. NO_3 and N_2O_5 were measured using a broadband cavity-enhanced absorption spectrometer (BBCEAS)[47] with a conservative limit of detection of 1 ppt. The height of the boundary layer was measured by a ceilometer.[48] Further information about the instrumentation can be found in the Supporting Information and in Shi et al.[35] The campaign average diurnal profile of NO_3 is shown in Figure 1e and those of isoprene and OH are shown in Figure 2C.[36] The meteorological variables of wind speed and direction, relative humidity, and temperature were measured at a height of 102 m on the IAP 325 m meteorological tower. Photolysis frequencies were calculated from the observed actinic flux using a spectral radiometer (Ocean Optics QE Pro spectrometer coupled to a 2π sr actinic receiver optic (Meteorologie Consult GmbH)). The naming structure for IN species follows Schwantes et al.,[25] with the general structure INX, where the position of N is the first number given and X represents other functional groups on the molecule and its position is given by the second number.

RESULTS AND DISCUSSION

Nitrate Radical Production and Loss. The comprehensive measurement suite available allows the investigation of the dominant production and loss mechanisms for NO_3 in Beijing. Figure 1a shows the mixing ratio of NO_3 radicals measured by the BBCEAS. The average NO_3 mixing ratio was 5 pptv, with a standard deviation of 10 pptv. A strong diurnal profile was observed, shown in Figure 1e, with a peak at 21:00−23:00 and a minimum around 06:00−08:00. The NO_3 production and loss rates were calculated using the measured O_3 and NO_2 concentrations and measurements of known NO_3 sinks,

including reaction with VOCs, photolysis, and loss via N_2O_5 heterogeneous uptake. More details on these calculations are provided in the SI. High ozone mixing ratios (up to 180 ppbv) in Beijing[35] resulted in high NO_3 production rates of the order of 4 ppbv h^{-1}, peaking in the late afternoon and early evening (Figure 1e). High daytime NO_3 loss rates, owing to rapid photolysis and reaction with NO, led to an average mixing ratio of ∼2 pptv of NO_3 into the afternoon (Figure 1e). It is often assumed that daytime reactions of NO_3 with hydrocarbons are negligible due to the dominance of loss processes over production. High levels of isoprene were observed in Beijing, shown in Figure 1b, with an average midday mixing ratio around 1 ppbv and a maximum of 2.7 ppbv, and so its reaction can compete as a NO_3 loss mechanism during the day. Figure 1c shows the fractional loss of NO_3 calculated from measurements of various NO_3 sinks; the absolute loss rates are also shown in Figure S3. Reaction with NO and photolysis dominate the loss rate of NO_3 in Beijing. The mean NO_3 loss to isoprene is around 5% across the entire measurement period (Figure 1d), but higher fractional loss rates were observed on some afternoons (Figure S4) with a maximum of 22% prior to sunset on June 14 (Figure S5).

Isoprene Nitrate Production. The main daytime sink of isoprene (ISOP) is its reaction with OH radicals, with the calculated loss rate of isoprene ($L_{ISOP+OH} = k_{OH}[OH][ISOP]$) peaking at about 3.7 ppbv h^{-1} at midday, as shown in Figure 2A. As a result of high day time emissions of isoprene, its loss rate via reaction with NO_3 ($L_{ISOP+NO_3} = k_{NO_3}[NO_3][ISOP]$) was highest between 13:00 and 18:00, as shown in Figure 2A, with a maximum loss rate of isoprene of 160 pptv h^{-1} in the afternoon. The loss of isoprene from reaction with O_3 was calculated to be a minor pathway, representing less than 10% of L_{ISOP} throughout the day.

The production rate of nitrates from isoprene can be estimated using eqs 1 and 2

$$P_{IsN\ ISOP+OH} = \alpha_1\, _1k\,[OH\ ISOP] \quad (1)$$

$$P_{IsN\ ISOP+NO_3} = \alpha_2 k_2[NO\ ISOP_3] \quad (2)$$

where α_1 and α_2 are the oxidant-specific relative yields of IsN, k_1 and k_2 are the rate constants for the reaction of isoprene with OH (1.0×10^{-10} cm^3 $molecule^{-1}$ s^{-1} at 298 K) and NO_3 (6.5×10^{-13} cm^3 $molecule^{-1}$ s^{-1} at 298 K), respectively.[50] During the afternoon in Beijing, Newland et al.[32] showed that the fraction of the peroxy (RO_2) radicals formed from isoprene + OH, reacting with NO can be as low as 65% (f_{NO} = 0.65), with the remainder reacting with HO_2, RO_2, or undergoing isomerization. Therefore, the production rate of IsN from OH chemistry calculated in eq 1 should be multiplied by f_{NO} during the afternoon as shown in eq 3. The hourly f_{NO} values used for Beijing were taken from Newland et al.[32]

$$P_{IsN\ ISOP+OH} = \alpha_1\, _1k\,[OH\ ISOP] \times f_{NO} \quad (3)$$

There is a degree of uncertainty in the values of the total first generation IsN yields, α_1 and α_2, in the literature, and a discussion of the recent literature is given in the SI, Section S4. We use α_1 = 0.11 from isoprene + OH/NO,[51] the most recent IUPAC recommended value,[50] and α_2 = 0.76 from isoprene + NO_3 from Schwantes et al.[25] (see the SI for discussion of values used here). A sensitivity analysis was also carried out using a range of α_1 and α_2 values, shown in the SI, but the overall trends in the IsN production are similar under all conditions The yield of IsN from the reaction of isoprene with O_3 is uncertain. The $P_{IN\ ISOP+O_3}$ was calculated following Liebmann et al.,[31] where the ozonolysis was assumed to lead to a 100% yield of RO_2 radicals and the OH IsN yield (α_1 = 0.11) was used. The total calculated IsN production rate ($P_{IsN\ total} = P_{IsN\ ISOP+OH} + P_{IsN\ ISOP+NO_3} + P_{IsN\ ISOP+O_3}$) is shown in Figure 2B, with a maximum of 535 pptv h^{-1} at 14:00. The relative contributions of the three pathways to $P_{IsN\ total}$ are shown in Figure S6. O_3 represents a minor pathway of IsN production in Beijing during the measurements, with an average $P_{IN\ ISOP+O_3}$ of 2.2% and a maximum of 5.8% at 18:00. Therefore, the following discussion focuses solely on the comparison of IsN production from reaction with OH and NO_3 radicals.

The calculated IsN production rates are shown in Figure 2B, with $P_{IsN\ ISOP+OH}$ shown in red and $P_{IsN\ ISOP+NO_3}$ shown in black. At midday, $P_{IsN\ total}$ is 480 pptv h^{-1}, with approximately 82% from the OH + NO chemistry ($P_{IsN\ ISOP+OH}$) and 16% from NO_3 oxidation ($P_{IsN\ ISOP+NO_3}$), as shown in Figure S6. The I-CIMS measured the sum of IHN ($C_5H_9NO_4$), the firstgeneration nitrates formed from isoprene + OH oxidation. The average diurnal observed is shown in black in Figure 2D, and peaked at midday at around 120 pptv, before dropping off in the late afternoon to a minimum overnight as isoprene was depleted.[36] By 16:00, $P_{IsN\ total}$ dropped to ca. 210 pptv h^{-1} as a result of the low-NO conditions in the afternoon and a reduction in the isoprene mixing ratios. At 16:00, 40% of the calculated $P_{IsN\ total}$ was from NO_3 + isoprene chemistry. Observations of δ-[1,4] and δ-[4,1]-isoprene carbonyl nitrates (INC) formed from NO_3 chemistry indicate that these species peak in the early evening (red line in Figure 2D). However, even though they are likely to undergo fast photolysis and rapid reaction with OH,[52] they are present during the daytime in low concentrations indicating daytime production of IsN from isoprene + NO_3 chemistry. A similar trend is seen in $C_5H_9NO_5$ (black line in Figure 2D), which is likely to be a mixture of IsN produced from NO_3 chemistry (isoprene nitrooxy hydroperoxide (INP), isoprene nitrooxy hydroxyepoxide (INHE), and isoprene dihydroxynitrate (IDHN)).[25] The mixing ratios of the IsN species will be controlled by a number of processes (secondary chemistry, photolysis, availability of co-reactants) and thus there is unlikely to be a direct correlation between them and the IsN production rate. The total mixing ratio of IsN observed was lower than the theoretical IsN production rate, likely as a result of loss processes and measurement of a small subset of potential IsN species.

Table 1. Molecular Formulae, Negative-Ion Masses ($[M - H]^{-1}$), Retention Times (RT), Time-Weighted Means (ng m^{-3}), Maximum and Minimum Concentration of NOS Observed in Beijing[a]

isoprene tracer	$[M - H]^{-1}$	RT (min)	time-weighted mean (ng m^{-3})	Max (ng m^{-3})	Min (ng m^{-3})	Ref
$C_5H_{11}O_9NS$	260.0082	0.86	12.6	154.1	0.10	19
$C_5H_9O_{10}NS$	273.9874	0.94	9.17	53.8	BD	47
C5H10O11N2S	304.9933	2.18	1.04	8.62	BD	19
C5H10O11N2S	304.9933	1.89	0.83	7.69	BD	19
C5H10O11N2S	304.9933	1.56	0.42	2.90	BD	19
C5H10O11N2S	304.9933	3.60	0.31	3.32	BD	19
$C_5H_9O_{13}N_3S$	349.9783	5.90	0.19	2.04	BD	25
$C_5H_9O_{13}N_3S$	349.9783	5.49	0.02	0.17	BD	25
$C_5H_9O_{13}N_3S$	349.9783	5.34	0.008	0.10	BD	25

a BD, below detection. The references indicate previous publications where these molecular formulae were observed in isoprene oxidation chamber experiments.

Even though only a small fraction of isoprene reacts with NO_3 during the afternoon (a few percent, as shown in Figure 2A), it can represent a significant source of IsN, contributing an average of 32% $P_{IsN\ total}$ over the afternoon (12:00−19:00). In the early evening and into the night, the contribution of $P_{IsN\ ISOP+NO_3}$ to the total $P_{IsN\ total}$ increases rapidly (average 86% between 19:00 and 05:00) as the photochemical production of OH drops significantly and NO_3 concentrations increase. Once produced, the gas-phase IsN can react further or partition into the particle phase either directly, depending on their volatility, or undergo heterogeneous uptake via the reaction with acidic particles, including the formation of nitrooxyorganosulfates (NOS). To study the presence of isoprene SOA in $PM_{2.5}$, we collected particles onto filters and analyzed the water-soluble extracts using UPLC-ESI-MS. This method is not particularly suited to IsN, owing to low signal intensity using ESI and the possibility of hydrolysis of IsN in aqueous solutions.

However, the sulfated analogues (NOS) give a strong signal and allow us to investigate the factors that can affect the production of SOA from isoprene nitrates in Beijing.

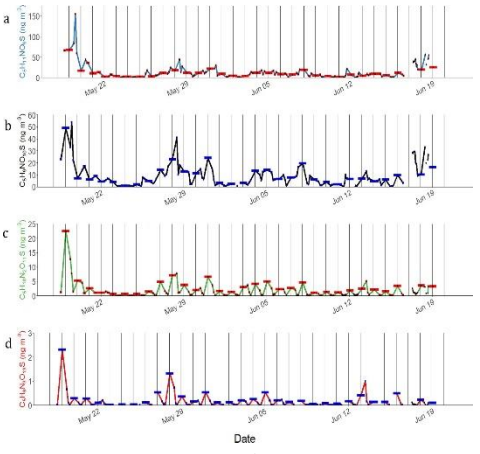

Fig 3. Time series of measured concentrations of NOS in Beijing aerosol. Vertical lines are midnight each day of sampling: (a) $C_5H_{11}NO_9S$ (MW 261), (b) $C_5H_9NO_{10}S$ (MW 275). (c) Sum of $C_5H_{10}N_2O_{11}S$ species (MW 306). (d) Sum of $C_5H_9N_3O_{13}S$ (MW 351) species. Blue and red bars on each point show full filter sampling time. Mid-sample points are connected with a line to show the temporal trend.

Particulate Isoprene Nitrooxyorganosulfates (NOS). Nine isoprene-derived NOS compounds were observed in the Beijing samples and their mean, median, and maximum observed concentrations are shown in Table 1. Two isoprenederived mono-nitrated tracers ($C_5H_{11}NO_9S$, molecular weight (MW) 261 and $C_5H_9NO_{10}S$, MW 275) followed similar temporal trends as other OS and with a strong correlation with particulate sulfate as discussed below.[36] Four isoprenederived di-nitrated NOS isomers ($C_5H_{10}N_2O_{11}S$, MW 306) and three tri-nitrated NOS isomers ($C_5H_9N_3O_{13}S$, MW 351) were also observed, all showing a strong enhancement during the night.

Mono-nitrate NOS. A NOS ($C_5H_{11}NO_9S$, MW 261) consistent with 2-methyltetrol nitrooxyorganosulfate was observed, and the time series is shown in Figure 3a. This species had a mean concentration of 12.6 ng m^{-3}, a standard deviation of 19.6 ng m^{-3}, and a maximum of 154 ng m^{-3}. This mean concentration is similar to that of 2-methyltetrol-OS (2MT-OS, MW 216) in $PM_{2.5}$, observed during the same period (mean = 11.8 ng m^{-3}, a standard deviation of 26.3 ng m^{-3}).

This species generally peaked in the samples taken during the late afternoon, as shown in box whisker plots in Figure 4A, although there is not a very strong diurnal profile. This NOS species was observed to have a moderate correlation with particulate sulfate (R^2 = 0.61) shown in Figure S7. This NOS species also correlated moderately to strongly with other OS species formed from isoprene oxidation by OH, observed in Beijing[36] (2-MT-OS, R^2 = 0.51; 2-methylglyceric acid-OS, R^2 = 0.58; $C_5H_{10}O_6S$, MW 198, R^2 = 0.80). Wang et al.[53] also observed that this NOS species correlated well with other isoprene-derived OS at Changping, a site 38 km northeast of Beijing. We propose that this NOS compound is formed from the acid-catalyzed heterogeneous uptake of isoprene nitrooxy hydroxyepoxide (INHE),[25] as shown in Scheme 1.

Scheme 1. Proposed Formation Pathways of Mono-Nitrated OS and Di-Nitrated OS Species Observed in the Aerosol from the NO_3 Initiated Oxidation of Isoprene[a]

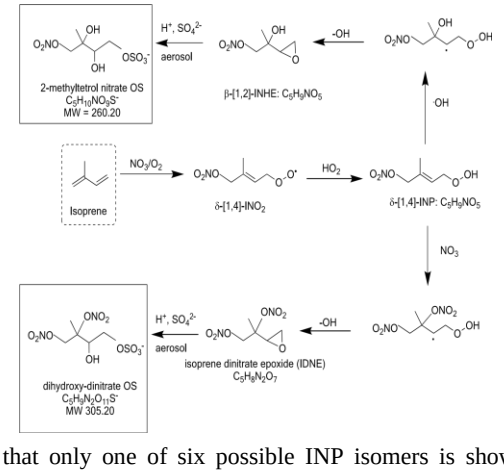

[a]Note that only one of six possible INP isomers is shown, for simplicity, with δ-[1,4]-INP and β-[1,2]-INHE the dominant isomers observed in Schwantes et al.[25]

The reaction of isoprene with NO_3 radicals leads to isoprene nitrooxy peroxy radicals (INO_2). Under the low concentrations of NO observed in this study, INO_2 can react with HO_2, leading to the formation of isoprene nitrooxy hydroperoxide (INP), as shown in the central section of Scheme 1. Using the observed concentrations of NO and HO_2 measured, we estimated that up to 10−15% of INO_2 can react with HO_2 during low NO afternoons in Beijing, as shown in Figure S8. There are six INP isomers possible and only the most abundant isomer (δ-[1,4]-INP) observed by Schwantes et al.[25] is shown. The reaction of INP with OH radicals, followed by OH recycling, can lead to INHE (β-[4,1]-INHE and β-[1,2]-INHE) in a similar way to the formation of isoprene-derived epoxydiols (IEPOX) from the reaction of OH with isoprene hydroxy hydroperoxides (ISOPOOH).[54] Schwantes et al.[25] also showed that INHE could undergo reactive uptake to highly acidified aerosol, similar to IEPOX.

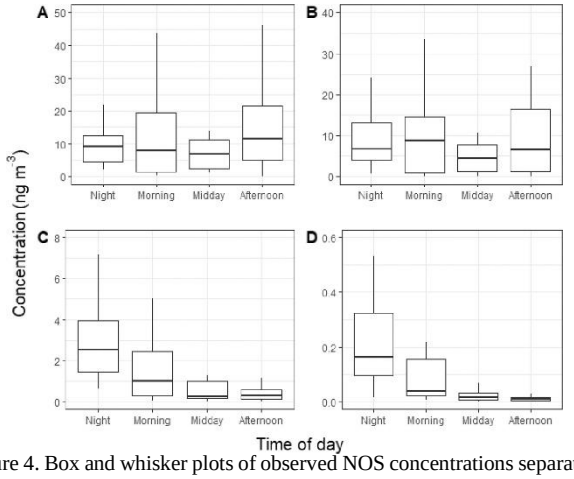

Figure 4. Box and whisker plots of observed NOS concentrations separated by the time of day the filter was collected: (A) $C_5H_{11}O_9NS$, (B) $C_5H_9O_{10}NS$, (C) $C_5H_{10}O_{11}N_2S$, and (D) $C_5H_9O_{13}N_3S$. The filter midpoints were split into different times of day, 00:00−07:00, 07:00−11:00, 11:00−13:00, and 13:00−17:00, based on the general sampling times of the filters (Table S2) and labeled as night, morning, midday, and afternoon, respectively. The thick black line represents the median value; the upper and lower hinges represent the 75th and 25th percentiles, respectively, with the upper and lower whiskers representing the largest value in the set. Outliers were removed so that the diurnal profiles could be seen more clearly.

reaction pathway to the formation of INHE). This ICN species can then react with NO_3 or OH, leading to the formation of the observed NOS species via an isoprene nitrooxy hydroxy-α-lactone (INHL) species, as shown in Scheme S1. This route is similar to the formation of 2methylglyceric acid (2-MG) from isoprene + OH derived hydroxymethyl-methyl-α-lactone (HMML).[16] The second proposed route is the formation of this species as a result of heterogeneous oxidation of 2-methyltetrol nitrate ($C_5H_{11}NO_9S$), as shown in Scheme S2. This route has recently been shown to be an important pathway to form the nonnitrated OS analogues, with 2-MT-OS undergoing saltingout to the surface of particles making it susceptible to heterogeneous OH oxidation.[55] The carbonyl species formed may then undergo cyclization to form a NOS hemiacetal species. Further work is needed to determine which of these pathways are important

for the formation of this abundant isoprene derived NOS species in polluted environments.

Di- and Tri-Nitrated NOS. Four of the isoprene-derived NOS species are di-nitrate isomers ($C_5H_{10}N_2O_{11}S$, MW 306, with retention times 1.56, 1.86, 2.18, and 3.6 min) and three are tri-nitrate isomers ($C_5H_9N_3O_{13}S$, MW 351, with retention times 5.34, 5.49, and 5.90 min). These structural isomers result from the different INO_2 radicals that can form during isoprene + NO_3 oxidation. However, the product-ion mass spectra (MS^2) provided only a few ions related to the loss of sulfate and nitrate and could not be used to determine the position of the groups. The time series of the sum of the diand tri-nitrated NOS is shown in Figure 3c,d, respectively. The sum of the four isoprene di-nitrate NOS isomers had an average concentration of 2.6 ng m^{-3}, a standard deviation of 2.6 ng m^{-3}, and a maximum of 23 ng m^{-3}. The tri-nitrated NOS species were observed at much lower concentrations, with an average sum of 0.2 ng m^{-3}, a standard deviation of 0.3 ng m^{-3}, and a maximum of 2.3 ng m^{-3}. These isoprenederived NOS exhibited moderate to strong correlations with each other, as shown in Figure S7 (R^2 = 0.76−0.99).

The di-nitrated NOS (MW 306) species show a strong enhancement at night, as shown in Figure 4C, with the mean nighttime concentration (3.43 ng m^{-3}), around 7 times higher than during the afternoon (0.47 ng m^{-3}). These NOS tracers have all previously been observed in chamber studies of NO_3 oxidation of isoprene.[19,25,50] The same di-nitrates have also been observed during the oxidation of isoprene by OH in the presence of NO,[58] but this is assumed to be a minor NOS formation pathway under the conditions observed in Beijing owing to their significant enhancement in the night-time samples. The tri-nitrated NOS is also elevated at night, as shown in Figure 4D, with very low concentrations observed in the afternoon.

Ng et al.[26] proposed the formation of di- and tri-nitrated OS via the formation of an isoprene hydroxynitrate (IHN) from INO_2 + INO_2 self-reactions after the initial NO_3 attack. A second NO_3 oxidation step at the other double bond then leads to the formation of dihydroxy-dinitrates, again via the reaction with INO_2 radicals. A subsequent unknown reaction step with particulate sulfate is then postulated to lead to NOS formation. Here, we propose an alternative mechanism where this species is formed via heterogeneous uptake of a dinitrated epoxide, as shown in the lower section of Scheme 1. Similar to the mono-nitrate formation, the NO_3 reaction with isoprene leads to INO_2, and the reaction with HO_2 leads to the isoprene nitrooxy hydroperoxide (INP). Subsequent addition of a second NO_3 at the C_2 position of the remaining double bond leads to an alkyl radical on the C_3 position. This radical then eliminates OH to form isoprene di-nitrated epoxide (IDNE), as proposed in Kwan et al.[57] Again, this mechanism is very similar to the production of IEPOX from ISOPOOH,[54] except in this case rather than being OH neutral (as in the mono-nitrate route to INHE in Scheme 1), it can act as a net source of OH radicals at night. Using an OH yield of 0.15, based on Wennberg et al.,[23] the calculated OH production rate from this pathway during sunset and early evening (19:00−22:00) was relatively small, of the order of 2−5 × 10^4 molecules cm^{-3} s^{-1}. The resulting IDNE species can then undergo heterogeneous uptake to acidic aerosols to form either di-hydroxy-di-nitrates via the reaction with H_3O^+ or di-nitrooxy hydroxy OS from the reaction with sulfate.

The isoprene-derived di- and tri-nitrated NOSs exhibited a strong diurnal profile as shown in Figure 4c,d, peaking in the night-time samples, suggesting their formation is a result of multiple steps of NO_3 oxidation. This is in contrast to the INHE-derived mono-nitrate outlined above that formed as a result of NO_3 oxidation followed by OH oxidation. The correlation of the di- and tri-nitrated NOS with particle sulfate is much weaker than the mono-nitrated NOS, as shown in Figure S7 (R^2 = 0.07−0.45). There is no correlation with the average night-time NO_3 mixing ratio (R^2 = 0.10), but there is a weak correlation with the maximum production rate of NO_3 (P_{NO_3}, R^2 = 0.29) calculated during each filter sampling period. Production of these NOS species is predicted to be highest just after sunset (ca. 19:15−19:30), where residual isoprene can react with increased levels of NO_3 as shown in Figure 1e, resulting from lower levels of photolysis. The production will then reduce rapidly as the isoprene and NO_3 are consumed, with the mean NO_3 dropping to sub-pptv values by 05:00 (see Figure 1e). The strong enhancement of the observed di- and tri-nitrated NOS at night, in comparison to the INHE-related mono-nitrate, may indicate that their common precursor INP reacts with OH radicals during the day, and the products that require two NO_3 oxidation steps therefore only form when OH levels drop after sunset. The formation route of the tri-nitrated species remains uncertain.

The diurnal profile of the di- and tri-nitrated NOS species both show a surprisingly rapid drop in the concentration during the daytime. In a previous study of highly oxidized organic nitrates using CIMS, the optimum model-observation agreement was achieved using a short atmospheric lifetime of the order of 2−4 h.[29] Therefore, the diurnal profile seen in Beijing is likely the result of a rapid in-particle loss of di- and tri-nitrated NOS, through processes such as hydrolysis or oxidation.[59,60] This may lead to particle-phase inorganic nitrate formation and act as a minor sink of atmospheric NO_x in Beijing. The drop in concentration of these species during the day may be partly due to the expansion of the boundary layer in the morning; however, this is not sufficient to explain the trends. On most days, there was also an appreciable amount of these NOS species in the morning samples, as shown in Figure 3c; and on a few days, the concentration of di-nitrated OS (MW 306) increased in the morning sample. The average diurnal profile of the observed mixing layer height during the campaign shows a shallow nocturnal boundary layer with a minimum of around 250 m at midnight, then increasing from around 08:00 to a maximum of around 1000 m at 15:00 (Figure S9). A recent study has shown the efficient formation of IsN in a polluted residual layer over Sacrameto, California.[61] We suggest that the relatively high abundance of these species during the early morning sample may be the result of mixing down of regionally produced NOS from the nocturnal residual layer during the collapse of the nocturnal boundary layer (Figure S9).

Our observations show that the reaction of isoprene with NO_3 leads to the formation of isoprene-derived nitrates in both the gas and particle phases in Beijing and that the nitrate radical plays a key role in the formation of IsN both during the day and at night. The mono-nitrated isoprene NOS identified are predominately formed in the late afternoon from the reaction with NO_3 and then OH radicals, with their concentration also influenced strongly by particulate sulfate availability. In contrast, the abundance of the di- and trinitrated isoprene NOS species, in summertime, is driven by both local night-time NO_3 chemistry, most likely in the early evening when the nitrate radical concentrations are increasing (and OH decreasing) as the sun goes down and isoprene is still present in reasonable amounts, and the mixing down of aged aerosol in the morning from more regional sources as the nocturnal boundary layer collapses. Unfortunately, the long nocturnal filter sampling time (15 h) in this study does not allow the full dynamics of the night-time formation of NOS to be observed and increased temporal resolution is needed to determine the relative role of isoprene, NO_3, and sulfate aerosol to and NOS formation in Beijing and other megacities. The measurements were taken at 8 m and so represent surface processes close to the emission of both isoprene and NO. Further work is needed to understand the extent of this chemistry throughout the boundary layer and the role of nonlocal sources on the isoprene IsN and NOS.

Supporting Information is available at https://pubs.acs.org/doi/10.1021/acs.est.0c05689.

Field instrumentation (Section S1); offline analysis (Section S2); calculations of NO_3 production and loss (Section S3); isoprene nitrate yields used in PIsN calculations (Section S4); INO_2 reaction with HO_2 and NO (Section S5); median diurnal variation of NO_3 loss fraction calculated using measured NO_3 sinks, including photolysis and

heterogeneous losses (Figure S1); calculated percentage of IN production (Figure S2); NO_3 loss rate calculated using measured NO_3 sinks (Figure S3); probability density function of the loss fraction of NO_3 (Figure S4); fractional NO_3 loss rate on the 14/06/2017, calculated using measured NO_3 sinks (Figure S5); fractional contribution to the calculate IsN production rate (Figure S6); corplot containing the nitrooxy organosulfates measured by UPLC-MS^2, particulate sulfate measured via an aerosol mass spectrometer (AMS) and the product of ozone and sulfate (Figure S7); plot of $k_{HO_2}/(k_{HO_2}+k_{NO})$ (Figure S8); average diurnal profile of boundary layer height (Figure S9); reactants included in NO_3 loss calculation (Table S1); start, end and midpoint date times for the filters collected and analysed for this study (Table S2) (PDF)

Funding

This project was funded by the Natural Environment Research Council, the Newton Fund and Medical Research Council in the U.K., and the National Natural Science Foundation of China (NE/N00700X/1, NE/N00695X/1, NE/N006895/1, NE/N007190/1, NE/N006917/1, NE/ N006909/1). D.J.B., F.A.S., and E.J.S. acknowledge NERC

SPHERES Ph.D. studentships. A.W.M. acknowledges a NERC PANORAMA Ph.D. studentship. P.M.E acknowledges funding the European Research Council Grant ERC-StG-802685. The Orbitrap-MS was funded by a Natural Environment Research Council strategic capital grant, CC090. J.D.S. and T.C. acknowledge support from the United States National Science Foundation (NSF) under Atmospheric and Geospace (AGS) Grant 1703535.

ACKNOWLEDGMENTS

The authors acknowledge the support from Pingqing Fu, Zifa Wang, Jie Li, and Yele Sun from IAP for hosting the APHHBeijing campaign at IAP. They also thank Tuan Vu, Roy Harrison, Di Liu, and Bill Bloss from the University of Birmingham; Alastair Lewis, William Dixon, Marvin Shaw, and Stefan Swift from the University of York. Siyao Yue, Liangfang Wei, Hong Ren, Qiaorong Xie, Wanyu Zhao, Linjie Li, Ping Li, Shengjie Hou, and Qingqing Wang from IAP; Kebin He and Xiaoting Chen from Tsinghua University, and James Allan from the University of Manchester for providing logistic and scientific support for the field campaigns; and Avram Gold and Zhenfa Zhang from the University of North Carolina for providing the 2-MT-OS and 2-MG-OS.

REFERENCES

(1) WHO. 7 Million Premature Deaths Annually Linked to Air Pollution; World Health Organization, 2014; . 66, pp 37−39. https://www.who.int/mediacentre/news/releases/2014/airpollution/en/ (accessed June 21, 2018).

(2) United Nations. World Urbanization Prospects, The 2018 Revision; Department of Economic and Social Affairs Population Dynamics, 2018.

(3) Guenther, A.; Karl, T.; Harley, P.; Wiedinmyer, C.; Palmer, P. I.; Geron, C. Estimates of Global Terrestrial Isoprene Emissions Using MEGAN (Model of Emissions of Gases and Aerosols from Nature). Atmos. Chem. Phys. 2006, 6, 3181−3210.

(4) Huang, C.; Yang, J.; Lu, H.; Huang, H.; Yu, L. Green Spaces as an Indicator of Urban Health: Evaluating Its Changes in 28 MegaCities. Remote Sens. 2017, 9, No. 1266.

(5) Mo, Z.; Shao, M.; Wang, W.; Liu, Y.; Wang, M.; Lu, S. Evaluation of Biogenic Isoprene Emissions and Their Contribution to Ozone Formation by Ground-Based Measurements in Beijing, China. Sci. Total Environ. 2018, 627, 1485−1494.

(6) Edney, E. O.; Kleindienst, T. E.; Jaoui, M.; Lewandowski, M.; Offenberg, J. H.; Wang, W.; Claeys, M. Formation of 2-Methyl Tetrols and 2-Methylglyceric Acid in Secondary Organic Aerosol from Laboratory Irradiated Isoprene/NOx/SO 2/Air Mixtures and Their Detection in Ambient PM2.5 Samples Collected in the Eastern United States. Atmos. Environ. 2005, 39, 5281−5289.

(7) Kroll, J. H.; Ng, N. L.; Murphy, S. M.; Flagan, R. C.; Seinfeld, J. H. Secondary Organic Aerosol Formation from Isoprene Photooxidation. Environ. Sci. Technol. 2006, 40, 1869−1877.

(8) Kleindienst, T. E.; Edney, E. O.; Lewandowski, M.; Offenberg, J. H.; Jaoui, M. Secondary Organic Carbon and Aerosol Yields from the Irradiations of Isoprene and α-Pinene in the Presence of NO_x and SO_2. Environ. Sci. Technol. 2006, 40, 3807−3812.

(9) Surratt, J. D.; Murphy, S. M.; Kroll, J. H.; Ng, N. L.; Hildebrandt, L.; Sorooshian, A.; Szmigielski, R.; Vermeylen, R.; Maenhaut, W.; Claeys, M.; Flagan, R. C.; Seinfeld, J. H. Chemical Composition of Secondary Organic Aerosol Formed from the Photooxidation of Isoprene. J. Phys. Chem. A 2006, 110, 9665−9690.

(10) Surratt, J. D.; Kroll, J. H.; Kleindienst, T. E.; Edney, E. O.; Claeys, M.; Sorooshian, A.; Ng, N. L.; Offenberg, J. H.; Lewandowski, M.; Jaoui, M.; Flagan, R. C.; Seinfeld, J. H. Evidence for Organosulfates in Secondary Organic Aerosol. Environ. Sci. Technol. 2007, 41, 517−527.

(11) Surratt, J. D.; Lewandowski, M.; Offenberg, J. H.; Jaoui, M.; Kleindienst, T. E.; Edney, E. O.; Seinfeld, J. H. Effect of Acidity on Secondary Organic Aerosol Formation from Isoprene. Environ. Sci. Technol. 2007, 5363.

(12) Surratt, J. D.; Chan, A. W. H.; Eddingsaas, N. C.; Chan, M.; Loza, C. L.; Kwan, A. J.; Hersey, S. P.; Flagan, R. C.; Wennberg, P. O.; Seinfeld, J. H. Reactive Intermediates Revealed in Secondary Organic Aerosol Formation from Isoprene. Proc. Natl. Acad. Sci. U.S.A. 2010, 107, 6640−6645.

(13) Surratt, J. D.; Go′mez-Gonza′lez, Y.; Chan, A. W. H.; Vermeylen, R.; Shahgholi, M.; Kleindienst, T. E.; Edney, E. O.; Offenberg, J. H.; Lewandowski, M.; Jaoui, M.; Maenhaut, W.; Claeys, M.; Flagan, R. C.; Seinfeld, J. H. Organosulfate Formation in Biogenic Secondary Organic Aerosol. J. Phys. Chem. A 2008, 112, 8345−8378.

(14) Chan, M. N.; Surratt, J. D.; Chan, A. W. H.; Schilling, K.; Offenberg, J. H.; Lewandowski, M.; Edney, E. O.; Kleindienst, T. E.; Jaoui, M.; Edgerton, E. S.; Tanner, R. L.; Shaw, S. L.; Zheng, M.; Knipping, E. M.; Seinfeld, J. H. Influence of Aerosol Acidity on the Chemical Composition of Secondary Organic Aerosol from βCaryophyllene. Atmos. Chem. Phys. Discuss. 2010, 10, 29249−29289.

(15) Lin, Y. H.; Zhang, H.; Pye, H. O. T.; Zhang, Z.; Marth, W. J.; Park, S.; Arashiro, M.; Cui, T.; Budisulistiorini, S. H.; Sexton, K. G.; Vizuete, W.; Xie, Y.; Luecken, D. J.; Piletic, I. R.; Edney, E. O.; Bartolotti, L. J.; Gold, A.; Surratt, J. D. Epoxide as a Precursor to Secondary Organic Aerosol Formation from Isoprene Photooxidation in the Presence of Nitrogen Oxides. Proc. Natl. Acad. Sci. U.S.A. 2013, 110, 6718−6723.

(16) Nguyen, T. B.; Bates, K. H.; Crounse, J. D.; Schwantes, R. H.; Zhang, X.; Kjaergaard, H. G.; Surratt, J. D.; Lin, P.; Laskin, A.; Seinfeld, J. H.; Wennberg, P. O. Mechanism of the Hydroxyl Radical Oxidation of Methacryloyl Peroxynitrate (MPAN) and Its Pathway toward Secondary Organic Aerosol Formation in the Atmosphere. Phys. Chem. Chem. Phys. 2015, 17, 17914−17926.

(17) Shrivastava, M.; Andreae, M. O.; Artaxo, P.; Barbosa, H. M. J.; Berg, L. K.; Brito, J.; Ching, J.; Easter, R. C.; Fan, J.; Fast, J. D.; Feng, Z.; Fuentes, J. D.; Glasius, M.; Goldstein, A. H.; Alves, E. G.; Gomes, H.; Gu, D.; Guenther, A.; Jathar, S. H.; Kim, S.; Liu, Y.; Lou, S.; Martin, S. T.; McNeill, V. F.; Medeiros, A.; de Sa, S. S.; Shilling, J. E.; Springston, S. R.; Souza, R. A. F.; Thornton, J. A.; IsaacmanVanWertz, G.; Yee, L. D.; Ynoue, R.; Zaveri, R. A.; Zelenyuk, A.; Zhao, C. Urban Pollution Greatly Enhances Formation of Natural Aerosols over the Amazon Rainforest. Nat. Commun. 2019, 10, No. 1046.

(18) Glasius, M.; Bering, M. S.; Yee, L. D.; de Sa, S. S.; Isaacman-VanWertz, G.; Wernis, R. A.; Barbosa, H. M. J.; Alexander, M. L.; Palm, B. B.; Hu, W.; Campuzano-Jost, P.; Day, D. A.; Jimenez, J. L.; Shrivastava, M.; Martin, S. T.; Goldstein, A. H. Organosulfates in Aerosols Downwind of an Urban Region in Central Amazon. Environ. Sci.: Processes Impacts 2018, 20, 1546−1558.

(19) Rattanavaraha W.; Chu, K.; Budisulistiorini, SH.; Riva M.; Lin YH; Edgerton, E. S.; Baumann, K.; Shaw, S. L.; Guo, H.; King, L.; Weber, R. J.; Neff, M. E.; Stone, E. A.; Offenberg, J. H.; Zhang, Z.; Gold, A.; Surratt, J. D. Assessing the Impact of Anthropogenic Pollution on Isoprene-Derived Secondary Organic Aerosol Formation in PM2.5 Collected from the Birmingham, Alabama, Ground Site during the 2013 Southern Oxidant and Aerosol Study. Atmos. Chem. Phys. 2016, 16, 4897−4914.

(20) Budisulistiorini, S. H.; Li, X.; Bairai, S. T.; Renfro, J.; Liu, Y.; Liu, Y. J.; McKinney, K. A.; Martin, S. T.; McNeill, V. F.; Pye, H. O. T.; Nenes, A.; Neff, M. E.; Stone, E. A.; Mueller, S.; Knote, C.; Shaw, S. L.; Zhang, Z.; Gold, A.; Surratt, J. D. Examining the Effects of Anthropogenic Emissions on Isoprene-Derived Secondary Organic Aerosol Formation during the 2013 Southern Oxidant and Aerosol Study (SOAS) at the Look Rock, Tennessee Ground Site. Atmos. Chem. Phys. 2015, 15, 8871−8888.

(21) Xu, L.; Guo, H.; Boyd, C. M.; Klein, M.; Bougiatioti, A.; Cerully, K.

M.; Hite, J. R.; Isaacman-VanWertz, G.; Kreisberg, N. M.; Knote, C.; Olson, K.; Koss, A.; Goldstein, A. H.; Hering, S. V.; de Gouw, J.; Baumann, K.; Lee, S.-H.; Nenes, A.; Weber, R. J.; Ng, N. L. Effects of Anthropogenic Emissions on Aerosol Formation from Isoprene and Monoterpenes in the Southeastern US. Proc. Natl. Acad. Sci. U.S.A. 2015, 112, 37−42.

(22) Ng, N. L.; Brown, S. S.; Archibald, A. T.; Atlas, E.; Cohen, R. C.; Crowley, J. N.; Day, D. A.; Donahue, N. M.; Fry, J. L.; Fuchs, H.; Griffin, R. J.; Guzman, M. I.; Herrmann, H.; Hodzic, A.; Iinuma, Y.; Jimenez, J. L.; Kiendler-Scharr, A.; Lee, B. H.; Luecken, D. J.; Mao, J.; McLaren, R.; Mutzel, A.; Osthoff, H. D.; Ouyang, B.; PicquetVarrault, B.; Platt, U.; Pye, H. O. T.; Rudich, Y.; Schwantes, R. H.; Shiraiwa, M.; Stutz, J.; Thornton, J. A.; Tilgner, A.; Williams, B. J.; Zaveri, R. A. Nitrate Radicals and Biogenic Volatile Organic Compounds: Oxidation, Mechanisms, and Organic Aerosol. Atmos. Chem. Phys. 2017, 17, 2103−2162.

(23) Wennberg, P. O.; Bates, K. H.; Crounse, J. D.; Dodson, L. G.; McVay, R. C.; Mertens, L. A.; Nguyen, T. B.; Praske, E.; Schwantes, R. H.; Smarte, M. D.; St Clair, J. M.; Teng, A. P.; Zhang, X.; Seinfeld, J. H. Gas-Phase Reactions of Isoprene and Its Major Oxidation Products. Chem. Rev. 2018, 118, 3337−3390.

(24) Doughty, D.; Fuentes, J. D.; Sakai, R.; Hu, X. M.; Sanchez, K. Nocturnal Isoprene Declines in a Semi-Urban Environment. J. Atmos. Chem. 2015, 72, 215−234.

(25) Schwantes, R. H.; Teng, A. P.; Nguyen, T. B.; Coggon, M. M.; Crounse, J. D.; St. Clair, J. M.; Zhang, X.; Schilling, K. A.; Seinfeld, J. H.; Wennberg, P. O. Isoprene NO_3 Oxidation Products from the $RO_2 + HO_2$ Pathway. J. Phys. Chem. A 2015, 119, 10158−10171.

(26) Ng, N. L.; Kwan, A. J.; Surratt, J. D.; Chan, A. W. H.; Chhabra, P. S.; Sorooshian, A.; Pye, H. O. T.; Crounse, J. D.; Wennberg, P. O.; Flagan, R. C.; Seinfeld, J. H. Secondary Organic Aerosol (SOA) Formation from Reaction of Isoprene with Nitrate Radicals (NO3). Atmos. Chem. Phys. 2008, 8, 4117−4140.

(27) Ayres, B. R.; Allen, H. M.; Draper, D. C.; Brown, S. S.; Wild, R. J.; Jimenez, J. L.; Day, D. A.; Campuzano-Jost, P.; Hu, W.; de Gouw, J.; Koss, A.; Cohen, R. C.; Duffey, K. C.; Romer, P.; Baumann, K.; Edgerton, E.; Takahama, S.; Thornton, J. A.; Lee, B. H.; Lopez-Hilfiker, F. D.; Mohr, C.; Wennberg, P. O.; Nguyen, T. B.; Teng, A.; Goldstein, A. H.; Olson, K.; Fry, J. L. Organic Nitrate Aerosol Formation via NO3 + Biogenic Volatile Organic Compounds in the Southeastern United States. Atmos. Chem. Phys. 2015, 15, 13377−13392.

(28) Massoli, P.; Stark, H.; Canagaratna, M. R.; Krechmer, J. E.; Xu, L.; Ng, N. L.; Mauldin, R. L.; Yan, C.; Kimmel, J.; Misztal, P. K.; Jimenez, J. L.; Jayne, J. T.; Worsnop, D. R. Ambient Measurements of Highly Oxidized Gas-Phase Molecules during the Southern Oxidant and Aerosol Study (SOAS) 2013. ACS Earth Space Chem. 2018, 2, 653−672.

(29) Lee, B. H.; Mohr, C.; Lopez-Hilfiker, F. D.; Lutz, A.; Hallquist, M.; Lee, L.; Romer, P.; Cohen, R. C.; Iyer, S.; Kurten, T.; Hu, W.; Day, D. A.; Campuzano-Jost, P.; Jimenez, J. L.; Xu, L.; Ng, N. L.; Guo, H.; Weber, R. J.; Wild, R. J.; Brown, S. S.; Koss, A.; de Gouw, J.; Olson, K.; Goldstein, A. H.; Seco, R.; Kim, S.; McAvey, K.; Shepson, P. B.; Starn, T.; Baumann, K.; Edgerton, E. S.; Liu, J.; Shilling, J. E.; Miller, D. O.; Brune, W.; Schobesberger, S.; D'Ambro, E. L.; Thornton, J. A. Highly Functionalized Organic Nitrates in the Southeast United States: Contribution to Secondary Organic Aerosol and Reactive Nitrogen Budgets. Proc. Natl. Acad. Sci. U.S.A. 2016, 113, 1516−1521.

(30) Huang, W.; Saathoff, H.; Shen, X.; Ramisetty, R.; Leisner, T.; Mohr, C. Chemical Characterization of Highly Functionalized Organonitrates Contributing to Night-Time Organic Aerosol Mass Loadings and Particle Growth. Environ. Sci. Technol. 2019, 53, 1165− 1174.

(31) Liebmann, J.; Sobanski, N.; Schuladen, J.; Karu, E.; Hellen, H.; Hakola, H.; Zha, Q.; Ehn, M.; Riva, M.; Heikkinen, L.; Williams, J.; Fischer, H.; Lelieveld, J.; Crowley, J. N. Alkyl Nitrates in the Boreal Forest: Formation via the NO3-, OH- and O-3-Induced Oxidation of Biogenic Volatile Organic Compounds and Ambient Lifetimes. Atmos. Chem. Phys. 2019, 19, 10391−10403.

(32) Newland, M. J.; Bryant, D. J.; Dunmore, R. E.; Bannan, T. J.; Acton, W. J. F.; Langford, B.; Hopkins, J. R.; Squires, F. A.; Dixon, W.; Drysdale, W. S.; Ivatt, P. D.; Evans, M. J.; Edwards, P. M.; Whalley, L. K.; Heard, D. E.; Slater, E. J.; Woodward-Massey, R.; Ye, C.; Mehra, A.; Worrall, S.; Bacak, A.; Coe, H.; Percival, C.; Hewitt, C. N.; Lee, J.; Cui, T.; Surratt, J.; Wang, X.; Lewis, A.; Rickard, A.; Hamilton, J. Rainforest-like Atmospheric Chemistry in a Polluted Megacity. Atmos. Chem. Phys. Discuss. 2020, 1−18.

(33) Stutz, J.; Wong, K. W.; Lawrence, L.; Ziemba, L.; Flynn, J. H.; Rappenglück, B.; Lefer, B. Nocturnal NO3 Radical Chemistry in Houston, TX. Atmos. Environ. 2010, 44, 4099−4106.

(34) Brown, S. S.; Dube, W. P.; Bahreini, R.; Middlebrook, A. M.; Brock, C. A.; Warneke, C.; de Gouw, J. A.; Washenfelder, R. A.; Atlas, E.; Peischl, J.; Ryerson, T. B.; Holloway, J. S.; Schwarz, J. P.; Spackman, R.; Trainer, M.; Parrish, D. D.; Fehshenfeld, F. C.; Ravishankara, A. R. Biogenic VOC Oxidation and Organic Aerosol Formation in an Urban Nocturnal Boundary Layer: Aircraft Vertical Profiles in Houston, TX. Atmos. Chem. Phys. 2013, 13, 11317− 11337.

(35) Shi, Z.; Vu, T.; Kotthaus, S.; Harrison, R. M.; Grimmond, S.; Yue, S.; Zhu, T.; Lee, J.; Han, Y.; Demuzere, M.; Dunmore, R. E.; Ren, L.; Liu, D.; Wang, Y.; Wild, O.; Allan, J.; Acton, W. J.; Barlow, J.; Barratt, B.; Beddows, D.; Bloss, W. J.; Calzolai, G.; Carruthers, D.; Carslaw, D. C.; Chan, Q.; Chatzidiakou, L.; Chen, Y.; Crilley, L.; Coe, H.; Dai, T.; Doherty, R.; Duan, F.; Fu, P.; Ge, B.; Ge, M.; Guan, D.; Hamilton, J. F.; He, K.; Heal, M.; Heard, D.; Hewitt, C. N.; Hollaway, M.; Hu, M.; Ji, D.; Jiang, X.; Jones, R.; Kalberer, M.; Kelly, F. J.; Kramer, L.; Langford, B.; Lin, C.; Lewis, A. C.; Li, J.; Li, W.; Liu, H.; Liu, J.; Loh, M.; Lu, K.; Lucarelli, F.; Mann, G.; McFiggans, G.; Miller, M. R.; Mills, G.; Monk, P.; Nemitz, E.; O'Connor, F.; Ouyang, B.; Palmer, P. I.; Percival, C.; Popoola, O.; Reeves, C.; Rickard, A. R.; Shao, L.; Shi, G.; Spracklen, D.; Stevenson, D.; Sun, Y.; Sun, Z.; Tao, S.; Tong, S.; Wang, Q.; Wang, W.; Wang, X.; Wang, X.; Wang, Z.; Wei, L.; Whalley, L.; Wu, X.; Wu, Z.; Xie, P.; Yang, F.; Zhang, Q.; Zhang, Y.; Zhang, Y.; Zheng, M. Introduction to the Special Issue "In-Depth Study of Air Pollution Sources and Processes within Beijing and Its Surrounding Region (APHH-Beijing). Atmos. Chem. Phys. 2019, 19, 7519−7546.

(36) Bryant, D. J.; Dixon, W. J.; Hopkins, J. R.; Dunmore, R. E.; Pereira, K. L.; Shaw, M.; Squires, F. A.; Bannan, T. J.; Mehra, A.; Worrall, S. D.; Bacak, A.; Coe, H.; Percival, C. J.; Whalley, L. K.; Heard, D. E.; Slater, E. J.; Ouyang, B.; Cui, T.; Surratt, J. D.; Liu, D.; Shi, Z.; Harrison, R.; Sun, Y.; Xu, W.; Lewis, A. C.; Lee, J. D.; Rickard, A. R.; Hamilton, J. F. Strong Anthropogenic Control of Secondary Organic Aerosol Formation from Isoprene in Beijing. Atmos. Chem. Phys. 2020, 20, 7531−7552.

(37) Riva, M.; Chen, Y.; Zhang, Y.; Lei, Z.; Olson, N. E.; Boyer, H. C.; Narayan, S.; Yee, L. D.; Green, H. S.; Cui, T.; Zhang, Z.; Baumann, K.; Fort, M.; Edgerton, E.; Budisulistiorini, S. H.; Rose, C. A.; Ribeiro, I. O.; e Oliveira, R. L.; dos Santos, E. O.; Machado, C. M. D.; Szopa, S.; Zhao, Y.; Alves, E. G.; de Sa, S. S.; Hu, W.; Knipping, E. M.; Shaw, S. L.; Duvoisin Junior, S.; de Souza, R. A. F.; Palm, B. B.; Jimenez, J.-L.; Glasius, M.; Goldstein, A. H.; Pye, H. O. T.; Gold, A.; Turpin, B. J.; Vizuete, W.; Martin, S. T.; Thornton, J. A.; Dutcher, C. S.; Ault, A. P.; Surratt, J. D. Increasing Isoprene Epoxydiol-to-Inorganic Sulfate Aerosol Ratio Results in Extensive Conversion of Inorganic Sulfate to Organosulfur Forms: Implications for Aerosol Physicochemical Properties. Environ. Sci. Technol. 2019, 8682.

(38) Kenseth, C. M.; Hafeman, N. J.; Huang, Y.; Dalleska, N. F.; Stoltz, B. M.; Seinfeld, J. H. Synthesis of Carboxylic Acid and Dimer Ester Surrogates to Constrain the Abundance and Distribution of Molecular Products in α-Pinene and β-Pinene Secondary Organic Aerosol. Environ. Sci. Technol. 2020, 12829.

(39) Brüggemann, M.; van Pinxteren, D.; Wang, Y.; Yu, J. Z.; Herrmann, H. Quantification of Known and Unknown Terpenoid Organosulfates in PM10 Using Untargeted LC−HRMS/MS: Contrasting Summertime Rural Germany and the North China Plain. Environ. Chem. 2019, 16, 333.

(40) Le Breton, M.; Wang, Y.; Hallquist, Å. M.; Pathak, R. K.; Zheng, J.; Yang, Y.; Shang, D.; Glasius, M.; Bannan, T. J.; Liu, Q.; Chan, C. K.; Percival, C. J.; Zhu, W.; Lou, S.; Topping, D.; Wang, Y.; Yu, J.; Lu, K.; Guo, S.; Hu, M.; Hallquist, M. Online Gas- and Particle-Phase Measurements of Organosulfates, Organosulfonates and Nitrooxy Organosulfates in Beijing Utilizing a FIGAERO ToFCIMS. Atmos. Chem. Phys. 2018, 18, 10355−10371.

(41) Mills, G. P.; Hiatt-Gipson, G. D.; Bew, S. P.; Reeves, C. E. Measurement of Isoprene Nitrates by GCMS. Atmos. Meas. Tech. 2016, 1−24.

(42) Reeves, C. E.; Mills, G. P.; Whalley, L. K.; Acton, W. J. F.; Bloss, W. J.; Crilley, L. R.; Grimmond, S.; Heard, D. E.; Hewitt, C. N.; Hopkins, J. R.; Kotthaus, S.; Kramer, L. J.; Jones, R. L.; Lee, J. D.; Liu, Y.; Ouyang, B.; Slater, E.; Squires, F.; Wang, X.; WoodwardMassey, R.; Ye, C. Observations of Speciated Isoprene Nitrates in Beijing: Implications Isoprene Chemistry. Atmos. Chem. Phys. 2020, 1−52.

(43) Hopkins, J. R.; Jones, C. E.; Lewis, A. C. A Dual Channel Gas Chromatograph for Atmospheric Analysis of Volatile Organic Compounds Including Oxygenated and Monoterpene Compounds. J. Environ. Monit.

2011, 13, 2268.
(44) Huang, Z.; Zhang, Y.; Yan, Q.; Zhang, Z.; Wang, X. Real-Time Monitoring of Respiratory Absorption Factors of Volatile Organic Compounds in Ambient Air by Proton Transfer Reaction Time-ofFlight Mass Spectrometry. J. Hazard. Mater. 2016, 320, 547−555.
(45) Whalley, L. K.; Stone, D.; Dunmore, R.; Hamilton, J.; Hopkins, J. R.; Lee, J. D.; Lewis, A. C.; Williams, P.; Kleffmann, J.; Laufs, S.; Woodward-Massey, R.; Heard, D. E. Understanding in Situ Ozone Production in the Summertime through Radical Observations and Modelling Studies during the Clean Air for London Project (ClearfLo). Atmos. Chem. Phys. 2018, 18, 2547−2571.
(46) Whalley, L. K.; Furneaux, K. L.; Goddard, A.; Lee, J. D.; Mahajan, A.; Oetjen, H.; Read, K. A.; Kaaden, N.; Carpenter, L. J.; Lewis, A. C.; Plane, J. M. C.; Saltzman, E. S.; Wiedensohler, A.; Heard, D. E. The Chemistry of OH and HO2 Radicals in the Boundary Layer over the Tropical Atlantic Ocean. Atmos. Chem. Phys. 2010, 10, 1555−1576.
(47) Zhou, W.; Zhao, J.; Ouyang, B.; Mehra, A.; Xu, W.; Wang, Y.; Bannan, T. J.; Worrall, S. D.; Priestley, M.; Bacak, A.; Chen, Q.; Xie, C.; Wang, Q.; Wang, J.; Du, W.; Zhang, Y.; Ge, X.; Ye, P.; Lee, J. D.; Fu, P.; Wang, Z.; Worsnop, D.; Jones, R.; Percival, C. J.; Coe, H.; Sun, Y. Production of N2O5 and ClNO2 in Summer in Urban
Beijing, China. Atmos. Chem. Phys. 2018, 18, 11581−11597.
(48) Kotthaus, S.; Grimmond, C. S. B. Atmospheric BoundaryLayer Characteristics from Ceilometer Measurements. Part 1: A New Method to Track Mixed Layer Height and Classify Clouds. Q. J. R. Meteorol. Soc. 2018, 144, 1525−1538.
(49) Tham, Y. J.; Wang, Z.; Li, Q.; Wang, W.; Wang, X.; Lu, K.; Ma, N.; Yan, C.; Kecorius, S.; Wiedensohler, A.; Zhang, Y.; Wang, T.
Heterogeneous N2O5 Uptake Coefficient and Production Yield of ClNO2 in Polluted Northern China: Roles of Aerosol Water Content and Chemical Composition. Atmos. Chem. Phys. 2018, 18, 13155−13171.
(50) IUPAC Task Group on Atmospheric Chemical Kinetic Data Evaluation. http://iupac.pole-ether.fr/ (accessed April 17 , 2020).
(51) Jenkin, M. E.; Young, J. C.; Rickard, A. R. The MCM v3.3.1 Degradation Scheme for Isoprene. Atmos. Chem. Phys. 2015, 15, 11433−11459.
(52) Xiong, F.; Borca, C. H.; Slipchenko, L. V.; Shepson, P. B. Photochemical Degradation of Isoprene-Derived 4,1-Nitrooxy Enal. Atmos. Chem. Phys. 2016, 16, 5595−5610.
(53) Wang, Y.; Hu, M.; Guo, S.; Wang, Y.; Zheng, J.; Yang, Y.; Zhu, W.; Tang, R.; Li, X.; Liu, Y.; Le Breton, M.; Du, Z.; Shang, D.; Wu, Y.; Wu, Z.; Song, Y.; Lou, S.; Hallquist, M.; Yu, J. The Secondary Formation of Organosulfates under Interactions between Biogenic Emissions and Anthropogenic Pollutants in Summer in Beijing. Atmos. Chem. Phys. 2018, 18, 10693−10713.
(54) Paulot, F.; Crounse, J. D.; Kjaergaard, H. G.; Kurten, A.; St. Clair, J. M.; Seinfeld, J. H.; Wennberg, P. O. Unexpected Epoxide Formation in the Gas-Phase Photooxidation of Isoprene. Science 2009, 325, 730−733.
(55) Nestorowicz, K.; Jaoui, M.; Rudzinski, K. J.; Lewandowski, M.; Kleindienst, T. E.; Spolnik, G.; Danikiewicz, W.; Szmigielski, R. Chemical Composition of Isoprene SOA under Acidic and NonAcidic Conditions: Effect of Relative Humidity. Atmos. Chem. Phys. 2018, 18, 18101−18121.
(56) Chen,Y.; Zhang,Y.;Lambe, A.T.; Xu,R.; et al.
Heterogeneous Hydroxyl Radical Oxidation of Isoprene-EpoxydiolDerived Methyltetrol Sulfates: Plausible Formation Mechanisms of Previously Unexplained Organosulfates in Ambient Fine Aerosols. Environ. Sci. Technol. Lett. 2020, 7, 460−468.
(57) Kwan, A. J.; Chan, A. W. H.; Ng, N. L.; Kjaergaard, H. G.; Seinfeld, J. H.; Wennberg, P. O. Peroxy Radical Chemistry and OH Radical Production during the NO_3-Initiated Oxidation of Isoprene. Atmos. Chem. Phys. 2012, 12, 7499−7515.
(58) Schwantes, R. H.; Charan, S. M.; Bates, K. H.; Huang, Y.; Nguyen, T. B.; Mai, H.; Kong, W.; Flagan, R. C.; Seinfeld, J. H. LowVolatility Compounds Contribute Significantly to Isoprene Secondary Organic Aerosol (SOA) under High-NOx Conditions. Atmos. Chem. Phys. 2019, 19, 7255−7278.
(59) Cole-Filipiak, N. C.; O'Connor, A. E.; Elrod, M. J. Kinetics of the Hydrolysis of Atmospherically Relevant Isoprene-Derived Hydroxy Epoxides. Environ. Sci. Technol. 2010, 44, 6718−6723.
(60) Darer, A. I.; Cole-Filipiak, N. C.; O'Connor, A. E.; Elrod, M. J. Formation and Stability of Atmospherically Relevant IsopreneDerived Organosulfates and Organonitrates. Environ. Sci. Technol. 2011, 45, 1895−1902.
(61) Zaveri, R. A.; Shilling, J. E.; Fast, J. D.; Springston, S. R. Efficient Nighttime Biogenic SOA Formation in a Polluted Residual Layer. J. Geophys. Res.: Atmos. 2020, DOI: 10.1029/2019JD031583.